Structural, electrical and magnetic characterisation of a new Aurivillius phase Bi5−xThxFe1+xTi3−xO15 (x = 1/3)

ARTICLE *in* JOURNAL OF ALLOYS AND COMPOUNDS · OCTOBER 2014

Impact Factor: 3 · DOI: 10.1016/j.jallcom.2014.04.045

5 AUTHORS, INCLUDING:

Valery G. Vlasenko
Research Institute of Physics
111 PUBLICATIONS **278** CITATIONS
SEE PROFILE

Sergey I. Levchenkov
Russian Academy of Sciences
106 PUBLICATIONS **243** CITATIONS
SEE PROFILE

Ya. V. Zubavichus
Kurchatov Institute
193 PUBLICATIONS **1,588** CITATIONS
SEE PROFILE

Journal of Alloys and Compounds 610 (2014) 184–188

Contents lists available at ScienceDirect

Journal of Alloys and Compounds

journal homepage: www.elsevier.com/locate/jalcom

Structural, electrical and magnetic characterisation of a new Aurivillius phase $Bi_{5-x}Th_xFe_{1+x}Ti_{3-x}O_{15}$ ($x = 1/3$)

V.G. Vlasenko [a,*], V.A. Shuvaeva [a], S.I. Levchenkov [b], Ya.V. Zubavichus [c], S.V. Zubkov [a]

[a] Southern Federal University, Research Institute of Physics, 344090 Rostov-on-Don, Russia
[b] Southern Federal University, Department of Chemistry, 344090 Rostov-on-Don, Russia
[c] National Research Center "Kurchatov Institute", 123182 Moscow, Russia

ARTICLE INFO

Article history:
Received 7 August 2013
Received in revised form 20 March 2014
Accepted 7 April 2014
Available online 18 April 2014

Keywords:
Aurivillius phases
X-ray powder diffraction
Dielectric properties
XAFS
Magnetic measurement

ABSTRACT

A novel Aurivillius oxide with the composition $Bi_{5-x}Th_xFe_{1+x}Ti_{3-x}O_{15}$ ($x = 1/3$) has been successfully prepared by the conventional solid-state high-temperature synthesis. X-ray diffraction confirmed that the material is strictly single-phase and has a four-layer Aurivillius structure with the orthorhombic lattice (unit cell parameters: $a = 5.4300(2)$ Å, $b = 5.4451(7)$ Å, $c = 41.2800(6)$ Å; space group $A2_1am$ (36)). Temperature dependent electrical and magnetic properties of the material have been investigated and compared to those of $Bi_5FeTi_3O_{15}$. The relative permittivity maximum and divergence of loss tangent, observed at 970 K, is attributed to a ferroelectric-to-paraelectric phase transition. At low temperature, the material exhibits paramagnetic behavior with short-range antiferromagnetic coupling. Analysis of Fe *K*-edge XAFS spectra showed that the Fe–O distances in $Bi_{5-x}Th_xFe_{1+x}Ti_{3-x}O_{15}$ ($x = 1/3$) are shorter and the general local environment of Fe is more distorted compared to $Bi_5FeTi_3O_{15}$. In both compounds the Fe atom is shifted from the center of the oxygen octahedron towards one of its faces, giving rise to three shorter and three longer Fe–O distances.

1. Introduction

The Aurivillius phases (AP) form a family of complex oxides, exhibiting a range of advanced dielectric properties, such as very high temperature of ferroelectric transition (often above 770 K), relatively high piezoelectric coefficients, strong anisotropic electromechanical coupling factors, high dielectric breakdown strengths and high stability. Therefore, APs are considered as promising materials for diverse applications, such as piezoactuators operated at extremely high temperatures [1,2].

Recently, APs bearing magnetic cations have drawn a special attention [3–16] due to their multiferroic nature, i.e., ability to display ferroelectricity and ferromagnetism simultaneously. The influence of preparation conditions, including doping with various elements, on the performance of the materials is a subject of many ongoing studies [17–21].

$Bi_5FeTi_3O_{15}$ (BFTO) is among most prospective and thus intensely studied multiferroic AP materials [8–12]. Its structure is formed by a four-layered perovskite unit of nominal composition $(Bi_3Ti_3FeO_{13})^{2-}$, sandwiched between $(Bi_2O_2)^{2+}$ layers along the *c* axis. BFTO is ferroelectric with a Curie temperature of about 1020 K [8], while its magnetic characteristics pose it as a superparamagnetic with the prevalence of antiferromagnetic coupling [9]. Weak ferromagnetism, presumably originated from Fe^{3+}/Fe^{2+} ions, has been also reported [10]. It has been claimed, that BFTO samples are characterized by diluted ferromagnetism due to a quite low volume fraction of magnetic ions. Non-linear magnetoelectric effect has been also observed for BFTO [12].

Crystallographic studies of BFTO [13–16] showed that Fe and Ti are randomly distributed over two available octahedral sites. However it has been pointed out that coordinates of atoms sharing the same crystallographic site cannot be unambiguously determined from diffraction data. So a study of local environment of Fe would be very useful for revealing the true position of Fe within the oxygen octahedron.

In this paper, we report a novel AP with the composition $Bi_{5-x}Th_xFe_{1+x}Ti_{3-x}O_{15}$ ($x = 1/3$) (BTFTO). As compared to BFTO, this material has a higher concentration of magnetoactive Fe ions due to a partial substitution of Bi^{3+} for Th^{4+} in the A perovskite sites. In this compound, both A and B sites are occupied by ions with different valences. The structural, dielectric and magnetic characteristics of the compound have been measured and compared to those of BFTO.

* Corresponding author. Tel.: +7 863 2223498.
E-mail address: v_vlasenko@rambler.ru (V.G. Vlasenko).

http://dx.doi.org/10.1016/j.jallcom.2014.04.045
0925-8388/

Furthermore, we also refined Fe–O distances in both compounds using XAFS data in order to get insight into the local coordination of the Fe atoms.

2. Experimental

2.1. Synthesis

Polycrystalline sample BTFTO was prepared by the conventional solid-state reaction of stoichiometric quantities of Bi_2O_3, TiO_2, Fe_2O_3 and $Th(OH)_4$. The substances were mixed, finely ground and pressed into pellets 10 mm in diameter and about 1 mm in thickness under the pressure of 20 MPa. The pellets then were fired in air for 3 h at 750–800 °C. After repeated grinding and pressing, the samples were sintered at 1020 °C for 2–3 h.

2.2. X-ray powder diffraction

X-ray powder diffraction data were collected using a 350-mm powder diffractometer at the Siberian Synchrotron Radiation Centre (Novosibirsk, Russia). The storage ring VEPP-3 with an electron beam energy of 2 GeV and a current of 70–90 mA has been used as the X-ray source. The XRD data were collected over the 2θ range of 0–160 deg. The wavelength of the incident beam was 1.097 Å. Unit cell parameters were refined by a least-squares routine implemented in the PCW-2.4 program [22].

2.3. XAFS data

The Fe *K*-edge EXAFS spectra for BTFTO and BFTO were obtained at the "Structural Materials Science" beamline of the Kurchatov Synchrotron Radiation Source (NRC "Kurchatov Institute", Moscow, Russia). The storage ring with electron beam energy of 2.5 GeV and a current of 70–90 mA was used as the source of radiation. All the spectra were recorded in the transmission mode using a Si(1 1 1) channel-cut monochromator and two ionization chambers filled with appropriate N_2/Ar mixtures. EXAFS data were analyzed using the IFEFFIT data analysis package [23]. The radial pair distribution functions around the Fe atoms were obtained by the Fourier transformation of the k^2-weighted EXAFS functions over the range of photoelectron wave numbers 2.8–12.0 $Å^{-1}$. The structural parameters, including interatomic distances, coordination numbers, and Debye–Waller factors were found by the non-linear fit of theoretical spectra to experimental ones. Theoretical spectra were simulated by means of FEFF7 [24].

2.4. Dielectric measurement

For dielectric measurements surfaces of the ceramic pellets were polished, covered with silver electrodes and fired at 750 °C. The dielectric properties were measured by E7-20 LCR-meter at several frequencies (100–1000 kHz) in the temperature range 295–1200 K.

2.5. Magnetic measurement

The magnetic susceptibility of the sample has been measured by the Faraday method in the temperature range from 77.4 K to 300 K. $Hg[Co(CNS)_4]$ has been used as a reference sample for calibration.

3. Results and discussion

3.1. X-ray diffraction

The powder X-ray diffraction pattern of BTFTO is shown in Fig. 1. All the observed XRD peaks were indexed assuming the orthorhombic space group $A2_1am$ (36), which is typical for $n = 4$ Aurivillius phases. No extra peaks, corresponding to admixture phases, were found confirming the strictly single-phase character of the BTFTO sample. The refined unit cell parameters have been determined to be $a = 5.4300(2)$ Å, $b = 5.4451(7)$ Å, $c = 41.2800(6)$ Å, which are rather close to those of BFTO ($a = 5.4260(9)$ Å, $b = 5.4551(9)$ Å, and $c = 41.137(6)$ Å) [13]. The room temperature orthorhombic distortion, estimated using the expression: $(b-a)/(a+b)$, appeared to be considerably smaller than that in BFTO (1.39×10^{-3} compared to 2.75×10^{-3}) in spite of quite close tolerance factors of the compounds (0.947 vs. 0.95).

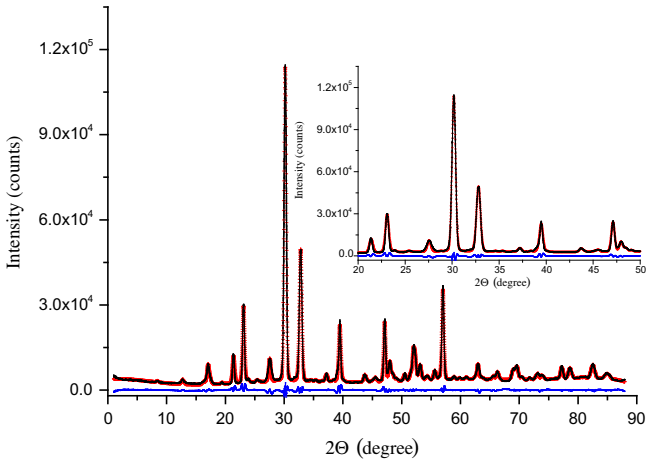

Fig. 1. Experimental (black line), calculated (red plus) and difference (blue line) powder X-ray diffraction patterns of BTFTO. (For interpretation of the references to colour in this figure legend, the reader is referred to the web version of this article.)

3.2. XAFS analysis

Fe *K*-edge XAFS spectra of the compounds were analyzed together with those of well-characterized FeO and Fe_2O_3, which were used as oxidation state references. Two independent probes, such as near-edge structure (XANES) and extended structure of absorption spectra (EXAFS), have been employed to determine the value and direction of Fe displacement off the centers of the oxygen octahedron.

It has been shown [25] that the 1s → 3d pre-edge region of Fe *K*-edge XAS spectra is highly sensitive to the geometry of the iron site since distortions, violating local inversion symmetry allow 3d-4p mixing, thereby increasing the intensity of the pre-edge feature. Besides the energy position of the edge was found to vary systematically with the oxidation state of the absorbing atom.

Fig. 2 shows the pre-edge region of Fe *K*-edge XANES spectra for BFTO, BTFTO as well as FeO and Fe_2O_3. The energy positions of the absorbing edges of BFTO, BTFTO and Fe_2O_3 are very close but differ from that of FeO by about 2 eV. This gives strong evidence, that the oxidation state of Fe atoms is 3+ in both APs. Quite noticeable pre-edge peaks **A**, observed in spectra of both BFTO and BTFTO compounds, indicate significant non-centrosymmetric distortions

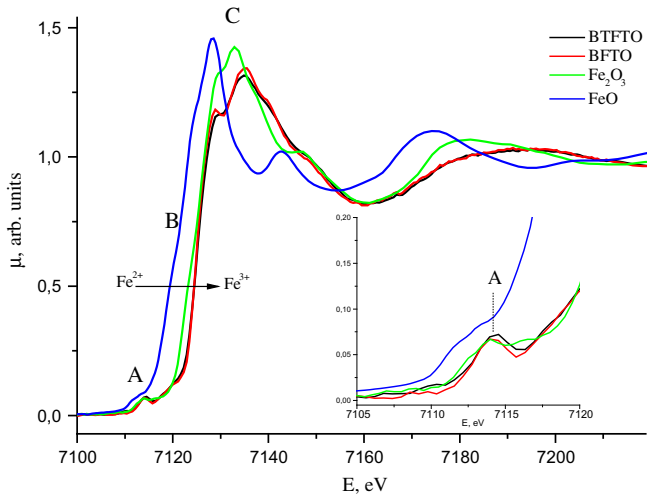

Fig. 2. XANES Fe *K*-edges of BTFTO, BFTO, Fe_2O_3 and FeO. The inset shows the pre-edge region of the absorbing edges.

of octahedral environment of the Fe atoms, originated from a Fe off-center displacement. A slightly higher intensity of the pre-edge peak in BTFTO, as compared to BFTO, indicates that the Fe environment therein is more distorted.

The Fourier transforms (FT) of the spectra, shown in Fig. 3, reveal a single major peak corresponding to Fe–O distances and a smaller one, originated from the Fe–Ti(Fe) coordination shell. The fitting was performed over the R range of 1.2–2.2 Å, which corresponds to the first peak of the experimental FT. The number of variable structural parameters was kept below the limit defined by the number of independent data points estimated by the formula $N_I = (2\Delta k \cdot \Delta r)/\pi + 2$.

Few fitting schemes have been tested. First, a fit has been made assuming that the major peak can be described with a unique Fe–O contribution. In the fitting procedure the distance (R), the Debye–Waller factor (σ^2), the coordination number (N), and the threshold energy shift (ΔE_0) values were allowed to vary. Thus the total number of variable parameters was 4 while the number of independent points was higher than 7. The results of the fit are presented in Table 1. It can be seen that the fit cannot be accepted as satisfactory since the best-fit coordination number for the shell was equal to 4, although it is well known, that Fe in all the samples has the octahedral oxygen environment. High values of the discrepancy factor and Debye–Waller factors σ^2 also indicate that the FT peak corresponds to several overlapping partly resolved Fe–O shells.

According to the structural data [26], there are three shorter and three longer Fe–O distances in the crystal structure of Fe_2O_3 and thus we selected such model for the next fit. Two shells with nonequivalent distances and coordination numbers set equal to 3 were refined. The distances obtained within this model for Fe_2O_3, appeared to be in a good agreement with those derived from crystallographic data. For BFTO the model also gave good results with Fe–O distances only by 0.03–0.04 Å shorter than those in Fe_2O_3. For both compounds, R and σ^2 were low. In BTFTO σ^2 appeared to be considerably higher than that in other compounds, indicating an additional distortion of the Fe local environment. The lower intensity of the Fe–Ti(Fe) peak in the FT XAFS of BTFTO, as compared to that of BFTO, is another evidence of higher structural distortion therein.

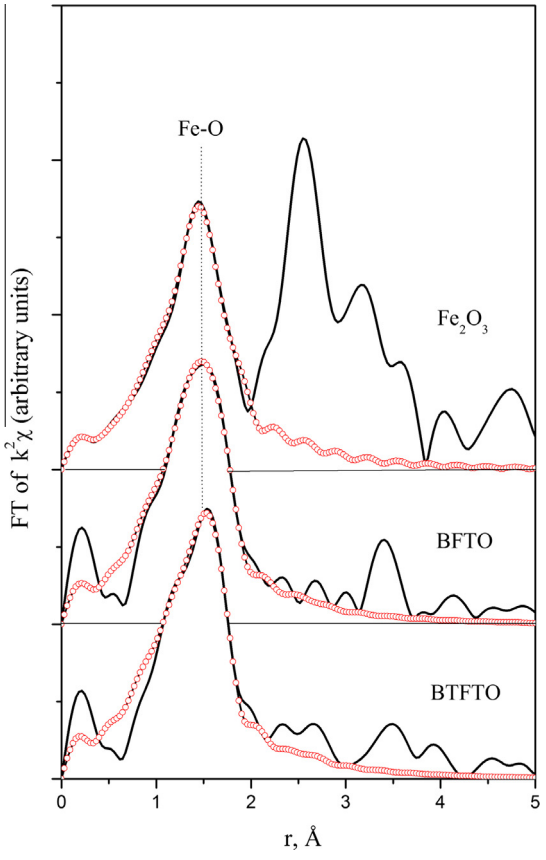

Fig. 3. Fourier transforms of the of BTFTO, BFTO and Fe_2O_3 (experiment – black line, theory – red open cycle). (For interpretation of the references to colour in this figure legend, the reader is referred to the web version of this article.)

Table 1
EXAFS best-fit parameters for the Fe-O shell in BTFTO, BFTO and Fe_2O_3.

Compound	R (Å)	N	σ^2 (Å^2)	Q[a] (%)
One-shell model				
Fe_2O_3	1.98	3.8	0.011	8.1
BFTO	1.98	3.7	0.011	6.6
BTFTO	1.98	3.4	0.012	6.0
Two-shell model				
Fe_2O_3	1.94	3	0.004	4.2
	2.08	3	0.005	
BFTO	1.91	3	0.004	2.5
	2.04	3	0.005	
BTFTO	1.90	3	0.006	3.8
	1.99	3	0.012	

[a] The quality of fits was estimated from the discrepancy factors Q between the experimental and simulated functions defined as: $Q(\%) = \frac{\sum[k\chi_{exp}(k) - k\chi_{th}(k)]^2}{\sum[k\chi_{exp}(k)]^2} \cdot 100\%$.

3.3. Dielectric characteristics

Fig. 4 shows the temperature dependence of dielectric constant $\varepsilon/\varepsilon_0(T)$ for BTFTO, measured at different frequencies (100–1000 kHz), which is quite typical of a ferroelectric material with a high conductivity, undergoing a diffuse phase transition. A broad frequency-independent high-temperature peak is observed at about 970 K in all $\varepsilon/\varepsilon_0(T)$ curves, which is most likely due to a ferroelectric–paraelectric phase transition. A divergence in the loss tangent curve, observed in the same temperature range, also gives a support to this interpretation. So, T_c for BTFTO appears to be lower than that in BFTO (1020 K [27]) in accordance with the lower room temperature orthorhombic distortion. Besides, the maximum of dielectric permittivity in BTFTO is substantially lower than that, reported for BFTO. Partially it may be due to the difference in sample characteristics such as density and grain size, which are crucial for the electrical performance of an AP material. So, compared to BFTO ferroelectric properties in FTFTO are suppressed. Previous studies [28,29] showed that rare-earth element substitution for Bi atoms at the A sites of perovskite layers results in a substantial degradation of ferroelectric properties, in particular, it gives rise to a decrease in T_c and maximum dielectric permittivity. Th atoms obviously induce a similar effect on ferroelectric properties.

As it can be seen from the inset in Fig. 4, a subtle dielectric anomaly is observed at about 510 K. A similar feature has been also reported for BFTO [10]. However its origin is still unclear.

The right panel of Fig. 4 shows the temperature variation of loss tangent ($\tan\delta$) at different frequencies in the range 100–1000 kHz for BTFTO compound. The anomaly in $\tan\delta$ is observed in the vicinity of Tc, which may be associated with the movement of ferroelectric domain walls. The dramatic increase of dielectric losses at high temperatures may be due to enhancement of conductivity of the sample.

The P–E hysteresis loop of the BTFTO ceramics is shown in Fig. 5. A high leakage current has not allowed us to apply electric field strong enough to saturate the loop, which has a roundish shape. However it still provides a clear evidence of ferroelectric properties of the sample. The real values of remnant polarization

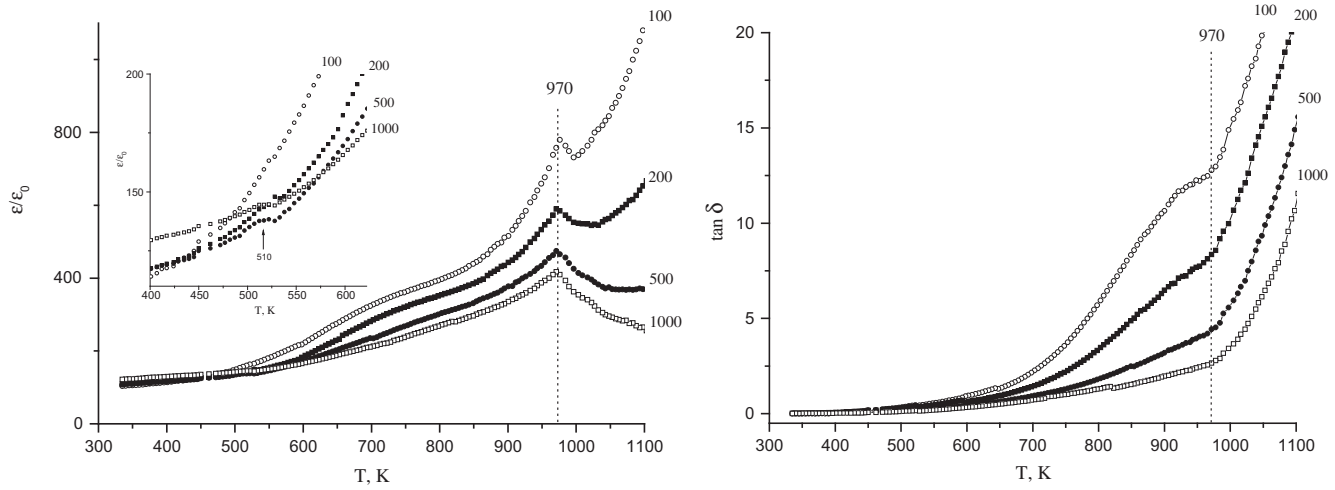

Fig. 4. Temperature dependence of the dielectric permittivity $\varepsilon/\varepsilon_0(T)$ (left panel) and the loss factor (right panel) of BTFTO measured at different frequencies (100–1000 kHz).

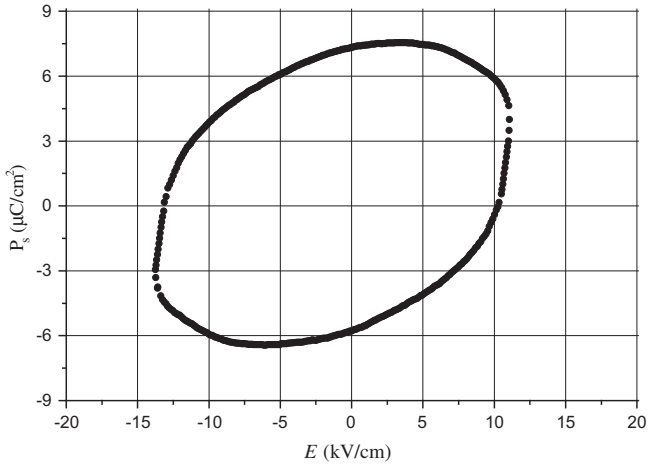

Fig. 5. Hysteresis loop of BTFTO measured at room temperature.

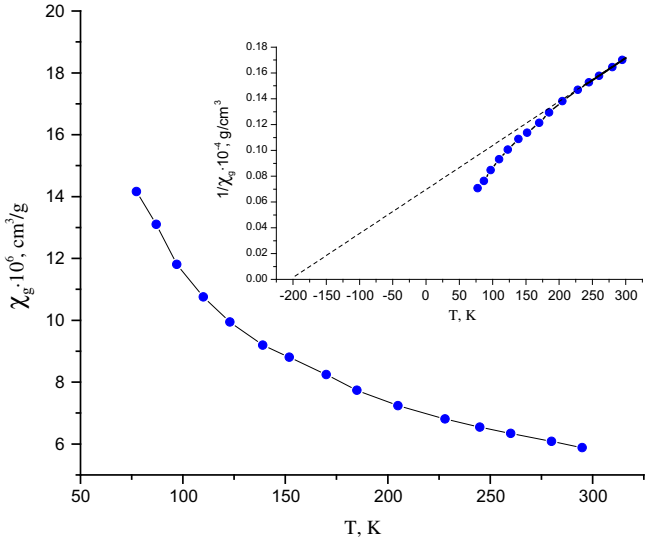

Fig. 6. Temperature dependence of magnetic susceptibility of BTFTO. The inset shows the low temperature magnetic inverse susceptibility data $1/\chi_g(T)$.

$(2P_r)$ and coercive field $(2E_c)$ of the sample should be well above the values of about 12.2 μC/cm^2 and 24 kV/cm respectively estimated from this unsaturated loop. It should be mentioned that the coercive field of BFTO, measured under driven electric field of 300 kV/cm, was reported to be 270 kV/cm, [10] which is much higher than the lower limit of the coercive field in our sample. However, the remnant polarization of our Th-doped sample appeared to be very close to that of BFTO (11.8 μC/cm^2).

3.4. Magnetic characteristics

Values of magnetic susceptibility for the BTFTO sample at 295 and 77 K were found to be 5.88×10^{-6} cm^3/g and 14.16×10^{-6} cm^3/g, respectively and the corresponding calculated magnetic moments per formula unit are 7.91 (1.98) and 6.28 (1.57) mB, which are considerably lower than 11.83 (2.94) as expected for spin-only magnetic moments of four Fe^{3+} ions. The lower value of low-temperature magnetic moment indicates antiferromagnetic coupling of paramagnetic centers. The temperature dependence of $1/\chi_g$ shown in Fig. 6 is typical of paramagnetic compounds with a short-range antiferromagnetic exchange coupling. Extrapolation of the curve measured above 150 K to the low temperature region yields a Weiss constant of -200 K. Similar temperature dependence of $1/\chi_g$ is observed for other Fe^{3+}-containing perovskite-like compounds. It should be noted that the Weiss constant for our sample is lower than that found for BFTO (160 K), which indicates that a higher Fe concentration results in enhanced antiferromagnetic coupling [9].

4. Conclusions

In summary, a partial Bi^{3+} substitution for Th^{4+} in the A perovskite sites in the promising multiferroic compound $Bi_5FeTi_3O_{15}$ allowed us to prepare a new material with the composition $Bi_{5-x}Th_xFe_{1+x}Ti_{3-x}O_{15}$ ($x = 1/3$), which has a higher concentration of magnetoactive Fe ions compared to BFTO. Th^{4+} has been chosen for doping as it has appropriate ion radius and allows to achieve a valence balance in Fe^{3+}-enriched BTFTO. The absence of phase impurities in the sample has been clearly proved by X-ray diffraction. Cell parameters have been refined within orthorhombic $A2_1am$ space group.

Fe local environment in BTFTO has been studied using Fe *K*-edge XAFS spectra and compared to that of BFTO and Fe_2O_3. The Fe off-center displacement in BTFTO appeared to be very close to that of BFTO in spite of stronger overall distortion of the structure.

Ferroelectric properties of the sample at room temperature have been confirmed by the P–E hysteresis loop. The T_c has been determined to be 970 K according to the position of the maximum on the relative permittivity versus temperature plot.

Magnetic performance of the material is typical of paramagnetic compounds with a short-range antiferromagnetic exchange. The Weiss constant, determined from temperature dependence of $1/\chi_g$, appeared to be lower than that of BFTO, indicating enhanced antiferromagnetic coupling.

Appendix A. Supplementary data

Supplementary data associated with this article can be found, in the online version, at http://dx.doi.org/10.1016/j.jallcom.2014.04.045.

References

[1] A. Moure, A. Castro, L. Pardo, Prog. Solid State Chem. 37 (2009) 15–39.
[2] B. Frit, J.P. Mercurio, J. Alloys Comp. 188 (C) (1992) 27–35.
[3] N. Sharma, B.J. Kennedy, M.M. Elcombe, Y. Liu, C.D. Ling, J. Phys.: Condens. Matter 20 (2) (2008). 025215 (6pp).
[4] N. Sharma, C.D. Ling, G.E. Wrighter, P.Y. Chen, B.J. Kennedy, P.L. Lee, J. Solid State Chem. 180 (1) (2007) 370–376.
[5] X. Mao, W. Wang, X. Chen, Y. Lu, Appl. Phys. Lett. 95 (8) (2009) 082901–0829013.
[6] M.A. Zurbuchen, R.S. Freitas, M.J. Wilson, P. Schiffer, M. Roeckerath, J. Schubert, M.D. Biegalski, G.H. Mehta, D.J. Comstock, J.H. Lee, Y. Jia, D.G. Schlom, Appl. Phys. Lett. 91 (3) (2007) 033113–0331133.
[7] A.R. James, G.S. Kumar, M. Kumar, S.V. Suryanarayana, T. Bhimasankaram, Mod. Phys. Lett. B 11 (14) (1997) 633–644.
[8] J.-B. Li, Y.P. Huang, G.H. Rao, G.Y. Liu, 1 J. Luo, J.R. Chen, J.K. Liang, Appl. Phys. Lett. 96 (2010) 222903.
[9] X.W. Dong, K.F. Wang, J.G. Wan, J.S. Zhu, J.-M. Liu, J. Appl. Phys. 103 (2008) 094101.
[10] X. Mao, W. Wang, X. Chen, Solid State Commun. 147 (2008) 186–189.
[11] G. Chen, W. Bai, L. Sun, J. Wu, Q. Ren, J. Appl. Phys. 113 (2013) 034901.
[12] A. Srinivas, S.V. Suryanarayana, G.S. Kumar, M. Kumar, J. Phys.: Condens. Matter 11 (16) (1999) 3335–3340.
[13] F. Kubel, H. Schmid, Ferroelectrics 129 (1992) 101–112.
[14] M. Krzhizhanovskaya, S. Filatov, V. Gusarov, P. Paufler, R. Bubnova, M. Morozov, D.C. Meyer, Z. Anorg. Allg. Chem. 631 (2005) 1603–1608.
[15] C.H. Hervoches, Ph. Lightfoot, Chem. Mater. 11 (1999) 3359–3364.
[16] C.H. Hervoches, A. Snedden, R. Riggs, S.H. Kilcoyne, P. Manuel, Ph. Lightfoot, J. Solid State Chem. 164 (2002) 280–291.
[17] G. Chen, W. Bai, L. Sun, J. Wu, Q. Ren, W. Xu, J. Yang, X. Meng, X. Tang, C.-G. Duan, J. Chu, J. Appl. Phys. 113 (2013) 034901.
[18] J. Dercz, J. Bartkowska, G. Dercz, P. Stoch, M. Łukasik, Int. J. Thermophys. 34 (2013) 567–574.
[19] J. Yang, W. Tong, Z. Liu, X.B. Zhu, J.M. Dai, W.H. Song, Z.R. Yang, Y.P. Sun, Phys. Rev. B 86 (2012) 104410.
[20] X. Chen, J. Xiao, Y. Xue, X. Zeng, F. Yang, P. Su, Ceram. Int. 40 (2014) 2635–2639.
[21] A. Kan, H. Ogawa, K. Kawada, T. Moriyama, Ferroelectrics 427 (2012) 129–136.
[22] W. Kraus, G. Nolze, Powder Cell for Windows, version 2.3, Federal Institute for Materials Research and Testing, Berlin, Germany, 1999.
[23] M. Newville, J. Synchrotron Radiat. 8 (2001) 96–100.
[24] S.I. Zabinski, J.J. Rehr, A. Ankudinov, R.C. Alber, Phys. Rev. B52 (1995) 2995–3009.
[25] T.E. Westre, P. Kennepohl, J.G. DeWitt, B. Hedman, K.O. Hodgson, E.I. Solomon, J. Am. Chem. Soc. 119 (1997) 6297–6314.
[26] E.N. Maslen, V.A. Streltsov, N.R. Streltsova, N. Ishizawa, Acta Crystallogr., B 50 (1994) 435–441.
[27] G.A. Geguzina, E.G. Fesenko, E.T. Shuvaeva, Ferroelectrics 167 (1995) 311–320.
[28] V.G. Vlasenko, A.T. Shuvaev, I.A. Zarubin, E.V. Vlasenko, Bull. Russ. Acad. Sci.: Phys. 73 (2009) 1134–1136.
[29] C. Long, H. Fan, P. Ren, Inorg. Chem. 52 (2013) 5045–5054.